Deformation Kinetics Analysis of Polymeric Matrices

Susan K. Lum[1] and Wendy C. Duncan-Hewitt[2,3]

Received January 29, 1996; accepted February 16, 1996

Purpose. We hypothesize that if the kinetics and the mechanisms involved in tablet compression are more fully understood and quantified, the parameters which influence tablet behavior in production may be controlled. The objective of our work was to obtain two deformation kinetic parameters for the predominant barrier to deformation, the activation volume (Vact) and the activation energy (Eact) of poly (methyl methacrylate-co-methacrylic acid) (PMMA/coMAA), a viscoelastic polymer similar to the commercial Eudragit©.

Methods. Stress relaxation studies were performed and monitored at varying temperatures on compacts using an instrumented Instron testing apparatus. Solid density, microindentation hardness and contact area testing served to quantify the shear stress rates.

Results. The Vact was found to be 64.4 ± 4 b^3, 63.8 ± 11 b^3, and 79.1 ± 8 b^3 for the applied strain rates of 1, 2, and 5 mm/min. The Eact for flow was determined to be 145 ± 7.7, 235 ± 8.0, and 506 ± 2.8 × 10^1kJ/mole^{-1} for the applied strain rates of 1, 2, and 5 mm/min respectively.

Conclusions. The average activation energies are indicative of strain hardening effects. The activation volumes and energies obtained will serve as estimates of these state variables for input into a particle deformation model of time-dependent compaction which is underway.

KEY WORDS: deformation kinetics; viscoelastic; activation barrier.

INTRODUCTION

All materials may be considered viscoelastic: they respond to stresses in a time-dependent manner. Quantitation of this "viscoelastic" behavior for pharmaceuticals is an essential component for the understanding of materials compaction. In tablet compaction, when stress is applied through the force of a punch, the elastic response of the constituent particles is instantaneous, whereas the viscous response is time dependent. For a highly viscous material with a low elastic modulus, rapid loading will favor large elastic strains; the molecules have no time to rearrange to a new position for flow. Hence, the residual elastic strain which results from the material's response to the applied stress will give rise to capping or lamination when this stress is released. Persistent tablet failure by lamination (horizontal splitting) during manufacturing or processing is a confounding and costly problem for process control.

Existing methods to quantify viscoelasticity of pharmaceutical materials, in general, provide only empirical fitted parameters that have not been validated by alternate means (1). They offer little insight into the physical basis for particle interaction.

Deformation kinetic analysis, which proposes that the flow of a solid is controlled by thermally activated phenomena, is an alternate means of quantifying viscoelasticity. It can be used as a modellistic link between the macroscopic observations of compact behavior and the properties of single constitutive particles (2). Once the important kinetic parameters for a material are defined and measured, they can be used in a more elaborate, predictive model of time-dependent tablet compaction.

BACKGROUND

Kinetics Approach to Deformation

This approach is based on the principle that the elementary physical processes producing the deformation of any solid, are the breaking and mending of intermolecular bonds. Thus plastic flow and chemical reactions are essentially similar processes; they are both solely the consequence of breaking and establishing atomic bonds. Plastic deformation is then analogous to a chemical reaction in which the composition remains the same but the bond structure of the molecule changes.

In polymers the time-dependent plastic deformation is accomplished by the gliding of the molecular segments of the polymers. Energy barriers must first be overcome before this segmental motion may occur. The associated rate of activation may be found from the reaction rate theory of thermally activated processes. As developed by Eyring in 1936 through statistical mechanics, the absolute rate theory for chemical reactions may be used to describe the movement of the flowing segments or 'units' together. The implicit assumption was that these flow units move by overcoming energy barriers.

For many polymeric materials (3), the steady state plastic flow rate is controlled by activation over a single symmetrical energy barrier. The total energy and number of molecules in the system is characterized by Boltzmann statistics at an initial configuration. The probability, P_i of finding an atom in the energy state E_i is then (3),

$$P_i = \frac{e^{-E_i/kT}}{\sum_{\infty} e^{-E_i/kT}}, \qquad (1)$$

k is the Boltzmann constant & T absolute temperature °K of the system with N atoms in thermal equilibrium, the number of atoms in an activated state (where $E_i \geq E$ the energy potential barrier) is (3),

$$NP_i = N \frac{\sum_{E_i>E} e^{-E_i/kT}}{\sum_{i=0}^{\infty} e^{-E_i/kT}} = Ne^{-E/kT} \qquad (2)$$

At thermodynamic equilibrium, the probability of deformation by thermal activation alone is equal in all directions. If a force

[1] Faculty of Pharmacy, University of Toronto, 19 Russell Street, Toronto, Ontario, Canada.
[2] Assistant Dean, School of Pharmacy, Texas Tech, Amarillo, Texas.
[3] To whom correspondence should be addressed.

Abbreviations: ν, frequency of motion; $\dot{r}$, plastic deformation rate; $\dot{\gamma}$, shear strain rate; $\dot{\tau}$, shear stress rate; A, contact area; b, burgers vector; d, distance; *E*, energy potential barrier; Eact, activation energy; E_i, energy state; F, uniaxial applied force; k, Boltzmann constant; N, number of atoms in an activated state; N_f, N_b, number of atoms in the forward and backward direction; P_i, probability; R, radius of spheroid disc; σ, stress; T, absolute temperature; τ, shear stress; Tg, glass transition temperature; V_{act}, activation volume; VHN, hardness or Vickers hardness number. W, work.

0724-8741/96/0500-0692$09.50/0

is applied to a system, the barrier height changes by the amount equivalent to the associated work, W. In Figure 1, the slanting energy barrier is shown. The effect essentially decreases the height of the activation barrier in the forward direction and increases the height of the activation barrier in the backward direction. The respective number of atoms in the forward and backward directions are:

$$N_f = \frac{N}{2} e^{-(E-W)/kT} \qquad N_b = \frac{N}{2} e^{-(E+W)/kT} \tag{3}$$

More specifically, the difference would be the net number of atoms deforming:

$$N_f - N_b = \frac{N}{2} e^{-E/kT\{eW/kT - e^{-W/kT}\}} \tag{4}$$

and since $\sinh x = {}^1/_2\{e^x - e^{-x}\}$, Equation 4 now becomes:

$$N_f - N_b = Ne^{-E/kT} \sinh\left\{\frac{W}{kT}\right\} \tag{5}$$

By letting $\dot{r}$ be the average rate of an atom traversing the imaginary distance d across the barrier in the conventional forward motion, we obtain the familiar Arrhenius form,

$$\dot{r} = \nu de^{-E/kT} \sinh\left\{\frac{W}{kT}\right\} \tag{6}$$

where ν is the frequency of motion.

Work is related to the stress field. One may substitute the definition of stress, $\sigma = F/A$, into the definition of work, $W = F \times d$, where F is the uniaxial applied force, A is the contact area, d is the distance traversed across the barrier. We find that

$$W = \sigma \times A \times d \tag{7}$$

where the product $A \times d$ is the activation volume (V_{act}).

Moreover, the Bailey-Orowan constitutive relation links shear strain rate ($\dot{\gamma}$) of dislocation movement to plastic deformation rates ($\dot{r}$). Although this approach was based on dislocation theory, the argument is valid as well for polymers and ceramics (4).

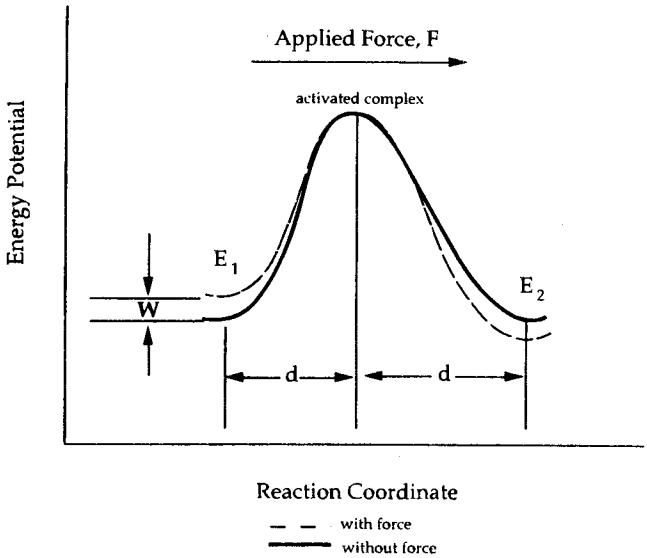

Fig. 1. The energy barrier of the flow unit as altered by an applied force.

Hence, rate of deformation at the microlevel may be expressed as

$$\dot{\gamma} = \nu de^{-E/kT} \sinh\left\{\frac{\sigma V_{act}}{kT}\right\} \tag{8}$$

If the forward motion dominates, as is likely under high stress conditions where activation barriers in the forward direction alone control deformation ($e\,\sigma V_{act}/kT > e\,-\sigma V_{act}/kT$), Equation 8 becomes

$$\ln \dot{\gamma} = \ln \nu - \frac{E}{kT} + \frac{\sigma V_{act}}{2kT} \tag{9}$$

At constant shear stress, one can evaluate the activation energy and volume for a given shear stress and temperature,

$$\left.\frac{\partial \ln \dot{\gamma}}{\partial kT}\right|_{\sigma} = -E_{act} \qquad \left.\frac{\partial \ln \dot{\gamma}}{\partial t}\right|_{T} = -V_{act} \tag{10}$$

The activation energy is associated with the height of the barrier whereas the activation volume is associated with the extent of the barrier to deformation.

From Phenomenological Model to Tablet Model

Thermal activation theory, as delineated above, defines energy potentials as a function of strain rate. The strain rate is not, however, directly measurable in a compaction experiment. By coupling a non-linear rheological model with activation rate theory, the strain rate may be replaced by the experimentally measurable shear stress rate.

Consisting of two linear springs and a dashpot in parallel configuration, the three element mechanical model with a non-Newtonian dashpot would represent the molecular processes associated with the deformation of polymers. In polymers, the extension of the spring is equivalent to the uncoiling of the polymer molecules from their random or equilibrium positions against the restoring tendency of the potential energy and entropy. The dashpot represents the slip of a molecule past its neighbors.

During stress relaxation, the strain rate of the non-linear dashpot must satisfy the condition that the total strain rate is equal to zero. Thus, the shear strain rate ($\dot{\gamma}$) in Equation 9 may be replaced by the shear stress rate ($\dot{\tau}$) to give:

$$\ln \dot{\tau} = \ln \nu - \frac{E}{kT} + \frac{\sigma V_{act}}{2kT} \tag{11}$$

While it is true that one can fit experimental data by using an infinite number of mechanical linear elements (5, 6), the viscoelastic constants derived thereby have no physical basis and are thus of no help in understanding the actual atomic processes underlying compaction. By simplifying the mechanical model to only a few elements to represent material behavior, it should be noted that each element is then representative of an entire spectrum of such arrangements for the material.

Normalization of Stress Curves

Stress relaxation varies with tablet porosity. In order to normalize the stress curves, a number of assumptions must be adopted. The interparticulate contact area must remain constant during stress relaxation. The shear stress imposed is further

assumed to be based on the von Mises yield criterion to convert the punch stress to shear stress

$$\tau = \frac{H}{3\sqrt{3}} \quad (12)$$

(VHN or H is the hardness of the material).

These assumptions and the justification for their adoption have been discussed at length elsewhere (7).

Deformation kinetic analysis has been applied and validated for a number of crystalline materials (1). Polymethylmethacrylate/comethacrylic acid (PMMA/coMAA) an amorphous acrylic polymer similar to the commercial pharmaceutical Eudragit® was chosen for study. Although the flow and materials behavior of polymethylmethacrylate (PMMA) alone is well documented, the copolymer material is more commonly employed in pharmaceutical coating and encapsulation processes, is markedly softer, and most importantly, can be directly compressed.

MATERIALS AND METHODS

Stress Relaxation

PMMA/coMAA spheres were prepared by free radical suspension polymerization of a mixture (50:50 wt%) of inhibitor-free methyl methacrylate (MMA) and inhibitor-free methacrylic acid (MAA) using recrystallized azo-isobutyrlnitrate (AIBN) as the initiator. The polymerization was carried out in a concentrated $CaCl_2$ solution at 70°C for 5–6 hours under nitrogen using freshly precipitated hydroxyapatite ($3Ca_3(PO_4).Ca(OH)_2$) as the suspending agent. The relative amount of monomer to water in the polymerization mixture was 1:8 by weight. After the completion of polymerization, the particles were filtered and then extracted in a soxhlet reflux with methanol for 2 days before being dried and fractionated. This removed residual monomer, catalyst and side products. For this study, fractions of PMMA/coMAA particles with a dry diameter of 0.6–0.85 mm were annealed at ~120°C for 2 hours prior to further testing. (Prepared by Dr. C. J. Kim, Temple University).

Compacts were made at temperature ranging from −25°C to 50°C since stress relaxation monitored at various temperatures permits the calculation of the activation energy. Prior to each compression, the stainless steel cylindrical die and flat faced punches (12mm diameter) were cleaned with methanol, lubricated with 1% magnesium stearate suspension, dried and filled with about 0.3g of PMMA/coMAA particles. An Instron (Model 4206) stress strain analyzer was electronically calibrated prior to each compression and used to manufacture compacts of varying relative density. The temperature control was provided by a mechanical cooling accessory (Dupont R #990476907-623), or by a feedback regulated heating tape (Thermolyne, Electrothermol regulator) and was monitored with calibrated thermocouples (J fine gauge Omega, Si heat sink compound for contact, amplifier and voltmeter circuitmate DM10 courtesy of Dr. R. List, Dept. of Physics, U of T).

The rate of punch displacement, or strain rate, ranged from 1 to 5 mm/min for compacts of final relative densities ranging from 0.66 to 1.00. At maximum punch travel (at loads of 62 to 93 kN), the movement of the crosshead was arrested and stress relaxation was monitored for 30 minutes. At least three runs were performed at each stress and strain level.

Here, we would like to underscore the fact that the rates and loads used in this study differ from those commonly employed in real tableting processes of powder mixtures. In general, real tableting processes occur in the 100–200 MPa range, while our configuration corresponds to approximately 500–800 MPa. This reflects the difference in the force required to directly compact our model polymeric material, to isolate material parameters, without the aid and complication of additional fillers and binders. The strain rates used were low, moreover, to facilitate accurate data acquisition of the stress response over a measurable interval. Our available equipment (Instron 4206 screw loaded) constrained our acquisition range.

Contact Area Change Under Stress Relaxation

The constancy of the contact area formed during stress relaxation is an essential assumption of this model. Concomitant measurement of this area change with time during stress relaxation was performed in an analogous series of stress relaxation tests.

Examination of the contact area between particles in the die, or even between two spheres in contact is difficult to achieve experimentally so the geometry was approximated by the contact of crossed cylinders at 90°. The contact zone of deformation between two crossed cylinders is geometrically analogous to the region of interest in particle-particle contact.

PMMA/coMAA rods ~1.2 cm diameter were prepared by thermal setting of the MMA and MAA monomers (1:1 mole ratio), degassed through repeated freeze thawing under an Argon blanket, combined with 0.5% (w/w) of AIBN initiator in glass molds at 70°C for 4 hours. The resulting cylinders were purified and annealed as described above for the copolymer particles prior to compaction under strain rates of 1 to 5 mm/min. At maximum punch travel (at loads of 3.0 to 4.5kN), the movement of the crosshead was arrested and stress relaxation was monitored for 30 minutes. High contrast photos (Nikon manual, 400 ASA Tmax black and white, custom 105 mm microscopic lens) were simultaneously taken of the contact zone at 90° to the axis of compression at 1 second intervals, processed, magnified and measured.

Microhardness Testing

Changes in material morphology and properties among sample matrices were monitored through microhardness testing. A small portion of the matrices were microtomed after swelling in MeOH/water (60/40) and subjected to static indentation. Using a Tukon miniload microindentation hardness tester (Model 300) equipped with a 136° Vickers and Knoop diamond pyramid indenter and microscope unit. The indenter was cleaned with acetone and allowed to dry. It was then lowered slowly onto the surface of the sample by a hydraulic mechanism over a period of 15s and the full load was maintained for 10s. The indenter was then raised automatically. Indentations were measured using the scale in the eyepiece of the microscope which was calibrated daily. The mean diameters of five indentations was used to calculate the average hardness values. The tests were performed at temperatures ranging from 25°C to 50°C to assess temperature-dependent flow.

For temperatures above 25°C, a microscope heating stage (Leitz 350) was installed on the tester and connected with a

circulating water bath (Polystat 1268-4). The temperatures were checked with the aforementioned thermocouple assembly which was connected directly to a stainless steel disc upon which the sample was mounted.

Polymer Characterization

Solid density measurements of the PMMA/coMAA particles were found using a stereopycnometer (purified helium gas, Quantachrome Stereopycnometer model SPV-2 #171, courtesy of Ortho-McNeil) and the Archimedes principle. After calibration with a stainless steel rod (volume 8.86 mL), the average density was determined after equilibration at various temperatures, to be modestly temperature dependent $\sim$1.25g/mL $-(0.002) \times$ temp(°C) SE = $\pm$0.001 g/mL. The glass transition temperature and melting characteristics were checked by differential scanning calorimetry (DSC, Perkin Elmer DSC-2). Repeated in quadruplicate, the scans showed a Tg $\sim$ 125°C and degradation above this temperature. The copolymer chains likely disentangled, thus permitting one monomer to volatilize (likely MMA which has a lower boiling point), as evidenced in the large endothermic peak and the loss in sample mass (reweighed PE Auto-2Z microbalance, error $\pm$ 2.0 $\times$ 10^1 μg, after scans). The temperature for subsequent annealing (within safety) is then $\sim$120°C.

The copolymer composition was checked by transmittance FTIR (Mattson #6020, courtesy of Dr. S. Balke, Dept. Chem. Eng., U of T). The polymer was first reprecipitated from acetone solution for further purification then film formed onto KBr (IR) discs from solution in methylene chloride. Scans showed that the copolymer was roughly 1:1 (at 3000 nm, ratio of peaks).

The size of the chains and the entanglement network involved in flow is dependent upon molecular weight. As such the viscosity average and weight average molecular weights were determined by capillary viscometry and by low angle laser light scattering (LALLS). Solutions of the copolymer ranging from 0.2 to 0.5% in freshly distilled THF were doubly filtered through 0.25μm PTFE filters to remove dust and other particulate matter. Firstly, the dn/dc or refractive index increment value was found using a Chromatix KMX-16 laser differential refractometer to be 0.1336 $\pm$ 1 $\times$ 10^{-5}. The viscosity average molecular weight was determined at 20°C to be 3.77 $\times$ 10^5 $\pm$ 6 $\times$ 10^4. (ECO Plastics capillary photodiiode viscometer). Light scattering was performed on a Chromatix KMAX-6 as a check, we found the Mw value to be of the same order of magnitude ($\sim$5 $\times$ 10^5). Thus our model amorphous glassy non-crosslinked acrylic copolymer is likely a highly entangled high molecular weight network.

RESULTS

Stress Relaxation

The data collected from the stress relaxation studies is summarized in Table I. Figure 2 illustrates the average force versus time plots for a set strain rate normalized by the procedures described in the introduction. When the stress relaxation curves at all relative densities were normalized and plotted using the Equations 10 described above, the plots were not collinear, contrary to our expectations.

Contacting Area Under Stress Relaxation

The resultant measurable change in contact area in the interaction zone between the two cylinders under deformation followed a monotonically increasing function. As depicted in Figure 3a and 3b, the particle-particle contact area peak and subsequent plateau corresponded with the peak measured contact stress. The plateau points were not significantly different within the experimental error (the precision was $\sim$2% on a calibrated test piece) as found by one way ANOVA. The contact area thus elucidated by this photomicroscopic method did not change during stress relaxation.

Microindentation Tests

Static Vicker's indentation hardness (VHN) tests were performed at various temperatures. The hardness of the polymer matrices decreased with temperature, VHN = 3153 $-$ 8.65 $\times$ temp (°K), SE = 1.46 p = 0.001, where the apparent hardness is corrected by the constraint factor 1.69. This was not unexpected, since increasing thermal energy translates as increased average internal energy: more molecules are able to overcome the energy barrier for flow. This further assesses the mechanical homogeneity of the materials among sample matrices. Changes in sample material morphology or properties would be reflected in these sample microindentation tests.

Table I. Summary of the Deformation Kinetic Data for PMMA/coMAA Compacts at 310°K

Sample #	Strain rate (mm/min)	Applied load (kN)	Weight (g)	Relative density	Slope of Ln (Shear strain rate) vs. avg shear stress	R^2	Activation volume (b^3)
1	1	65	0.3433	0.97	0.69	0.95	70
2	1	70	0.3292	0.99	0.63	0.93	63
3	1	71	0.2588	0.92	0.59	0.96	59
4	1	78	0.2157	0.79	0.66	0.96	66
5	2	68	0.3459	0.95	0.53	0.98	53
6	2	73	0.2551	0.95	0.74	0.92	74
7	2	78	0.2315	0.94	0.65	0.95	65
8	5	83	0.2664	0.96	0.86	0.94	86
9	5	89	0.2361	0.95	0.69	0.95	69
10	5	93	0.2555	1.00	0.82	0.91	82

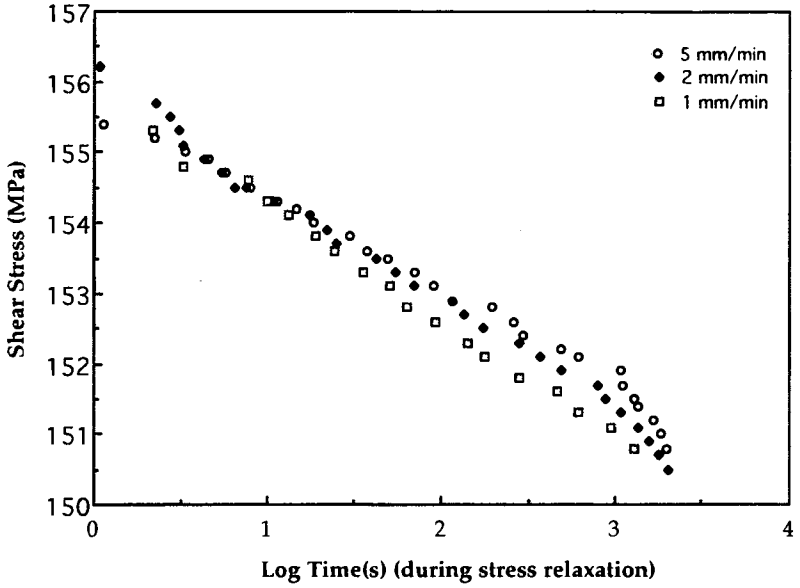

Fig. 2. Shear Stress versus time plots for the stress relaxation of PMMA/coMAA compacts compressed at various strain rates. Shear stress was calculated using the punch force and the hardness value for the sample. The rate of stress relaxation varies with compaction force and rate, as well as tablet relative density.

DISCUSSION

It is customary to express the activation volume for deformation in terms of Burgers vectors. The Burgers vector, b, is the unit deformation distance and often is equivalent to the dimension of the flow unit. It was proposed that with an amorphous glassy polymer, an applied stress field would create regions of shear analogous to dislocation loops (8). The Burgers vector is then the magnitude of the shear displacement in a sheared region. It should be emphasized however, that the dislocation analogy is simply a convenient tool for visualization and that the theoretical calculation by Eshelby (1957) (9) was developed without any direct reference to dislocations and their properties. He calculated the elastic strain energy of a sheared ellipsoidal region in an applied stress field and related the yield stress to the measured modulus of a sample:

$$W = -\frac{2}{3}\pi R^2 b\tau \qquad (13)$$

where W is the work done by an applied stress, R is radius of spheroid disc, τ is shear stress.

From shear modulus and compressive yield stress data obtained on carefully conditioned identical samples of PMMA, the b of the sheared regions was calculated to be approximately 3.5Å from $-120°$ to 80°C (10). This was the value used in subsequent calculations as there is a dearth of work performed on PMMA copolymers.

The activation energy for flow of the copolymer was determined to be 145 ± 7.7, 235 ± 8.0, and 506 ± 2.8 × 10^1kJ/mol^{-1} kJ/mol for the applied strain rates of 1, 2, and 5 mm/min respectively. This was calculated from data collected at varying temperatures using a plot of ln(stress rate at constant shear stress) as shown in Figure 4. This lack of collinearity may be indicative of the inadequacy of the simple assumption of constancy of contact stress/area used to normalize the stress curves.

The activation volume (64.4 ± 4 b^3, 63.8 ± 11 b^3, and 79.1 ± 8 b^3 for the applied strain rates of 1, 2, and 5 mm/min respectively, where b is the Burgers vector, 3.5Å as previously discussed) was calculated from plots of ln(shear stress rate) vs. shear stress using Equation 10b (Figure 5). Normalization was performed in order to compare the effect of strain rate and temperature trends in the same plot. The data for manipulation of the shear stress values for the activation volume and energy values does not require this explicit normalization by relative density. Literature values of Vact for this material are not available, but it is associated with the size of the deformation region.

Viscoelastic deformation, deformation which occurs as a combination of time independent (elastic) and time-dependent (viscous) processes, is exhibited by both crystalline and polymeric materials. It must be emphasized however that on a molecular level, viscoelastic flow occurs via very different paths. Within a crystalline lattice, dislocations or defects exist. The movement of such dislocations play an integral part in the deformation process. An amorphous, glassy polymer on the other hand, consists of an entangled network of long chain polymer molecules. For polymers above their glass transition temperature, the constant thermal motion (Brownian motion) of the polymer segments play a large part in explaining flow and deformation. Segments move by virtue of rotations around single bonds in the main chain of the polymer. As a result of thermal energy fluctuations, 'holes' covering a spectrum of volumes and involving segments of several polymer chains are continuously formed and destroyed. These microvoids are not fixed in space. Of the total energy of activation for viscous flow, only a small portion is required to articulate the segments. The major portion is used to form these 'holes' for the new equilibrium position (11).

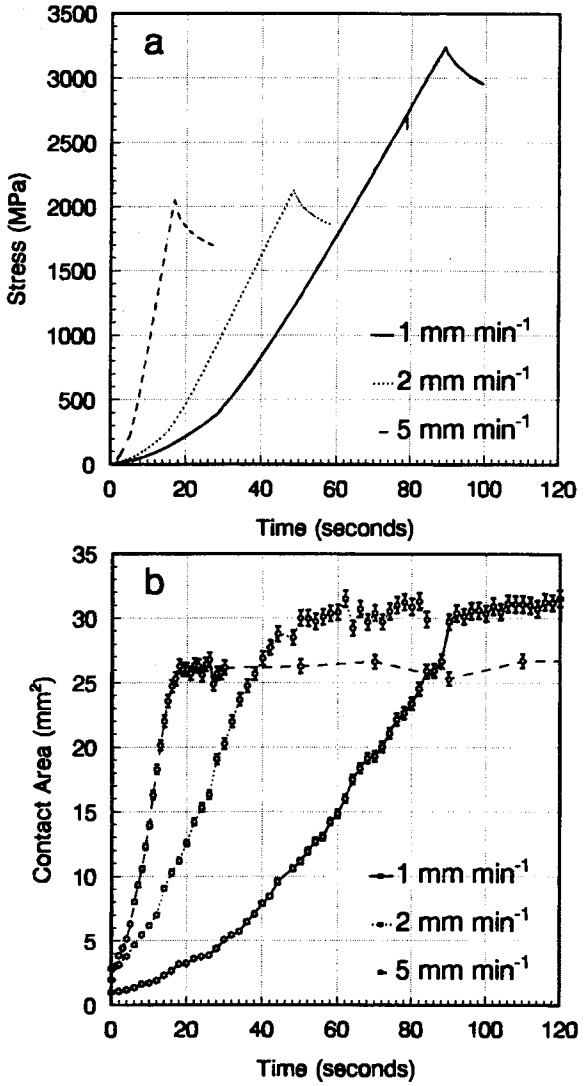

Fig. 3. Copolymer cylinders undergoing compactive loading (a) Plot of stress monitored with time during stress relaxation for peak load of 3.5kN (b) Concomitant measure of the interfacial contact area during stress relaxation.

When stressed initially, the copolymer stored this energy as elastic strain energy within bond angle and distance distortions. The temperature was below the Tg (the polymer segments did not have sufficient energy to move past one another) so no gross movement of the segments could occur. The local *in situ* contact temperature rose as compaction progressed. This was evidenced by our thermocouple monitoring of the outer die (a well for the fine gauge thermocouple was drilled at the halfway thickness of the die wall and at a depth equaling that of the compact). Such a thermal rise was not unexpected. Friction during compression may contribute to this increase. Under rapid compressive stress applications to PMMA samples (12), an adiabatic temperature change was observed and attributed by these authors to a thermoelastic effect as defined by the classical Thomson equation. A temperature rise of the order of 3° detected by an embedded thermocouple for a 200 MPa load on a large cylindrical sample (22 mm × 9.5 mm) was observed. On a local scale, subsequent plastic deformation under adiabatic conditions at reasonably high strain rates could lead to the observed increased local temperatures. This regime of adiabatic heating was identified in failure mechanism diagrams (13) for glassy PMMA under compression.

Once the glass transition temperature is surpassed, our copolymer segments can rearrange to relieve the applied stress. The polymer chains uncoil from their random conformations and rotate about single successive bonds to form the statistical segmental 'holes' for flow. The activation energy term then encompasses this intramolecular energy barrier to free rotation.

As alluded to earlier, stress relaxation within a compact is a function of porosity. By determining hardness values for all the temperatures employed in the stress relaxation tests, the stress curves were to be normalized. Unfortunately, normalization by this procedure did not give rise to collineation of the stress curves as shown in Figure 2. In this case, it becomes necessary to redress the assumptions implicit in the tablet model incorporating activation theory.

This model was based on the assumption that the interparticulate contact area generated during compaction does not change during stress relaxation. This assumption can be justified since compaction imposes strain not stress on the contents of the die. In this configuration, a given displacement was imposed on the contents of the die, so that once the movement of the punch ceased, the particles were no longer compelled to approach one another which is the driving force for contact area enlargement.

To further assess this essential assumption, the contacting surface area of two crossed cylinders undergoing compactive loading under similar rates was examined. The cylinders were used in a crossed geometry akin to that of surface force measurements in order to minimize point loading effects. The contact area plateaus with peak stress as shown in Figure 3b, which lends support to the criterion of constant contact area under stress relaxation. The contact stress per area relation may however complicate the stress relaxation.

It was assumed that the yield behavior was independent of the strain history. If strain hardening occurred, then the contact stress/area relationship would no longer be constant and would result in nonoverlap of the normalized relaxation curves. As evidenced in Figure 5, the normalized slope of the stress relaxation plot is a function of compaction force which is an indication of strain hardening. Moreover, the activation energies obtained for different strain rates are a function of the loading rate.

Under uniaxial compressive loading conditions, the underlying polymeric network chain structure undergoes a planar orientation process which may in part account for the observed increase of the experimental activation volumes and energies with increasing relative densities. The copolymer strain hardened. Paradoxically, glassy polymers are often cited for displaying strain softening (14) in tensile tests. The contact configuration cited in tensile materials testing however differs greatly from this compaction configuration wherein particles are subjected to large confined shear stresses. In tensile testing, constant strain rate tests must be used in order to accurately obtain the true material response; to uncouple strain softening phenomenon from the effects due to changing strain rate (15).

The activation volumes and energies obtained then are simply rough estimates of these state variables. They will serve as rough boundary value energy parameters for input into a

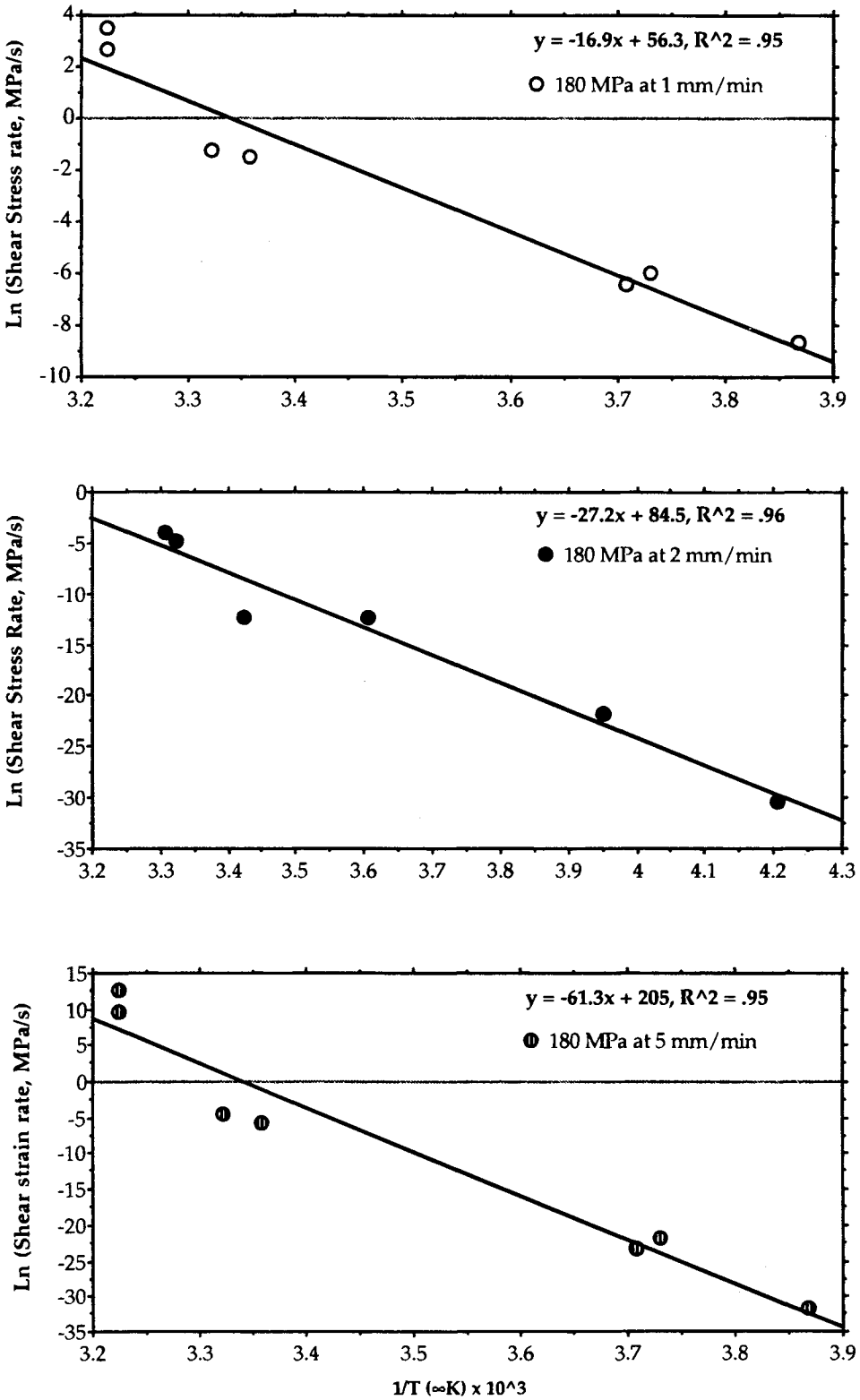

Fig. 4. Arrhenius plots for PMMA/coMAA particles for activation energy determinations at different strain rates.

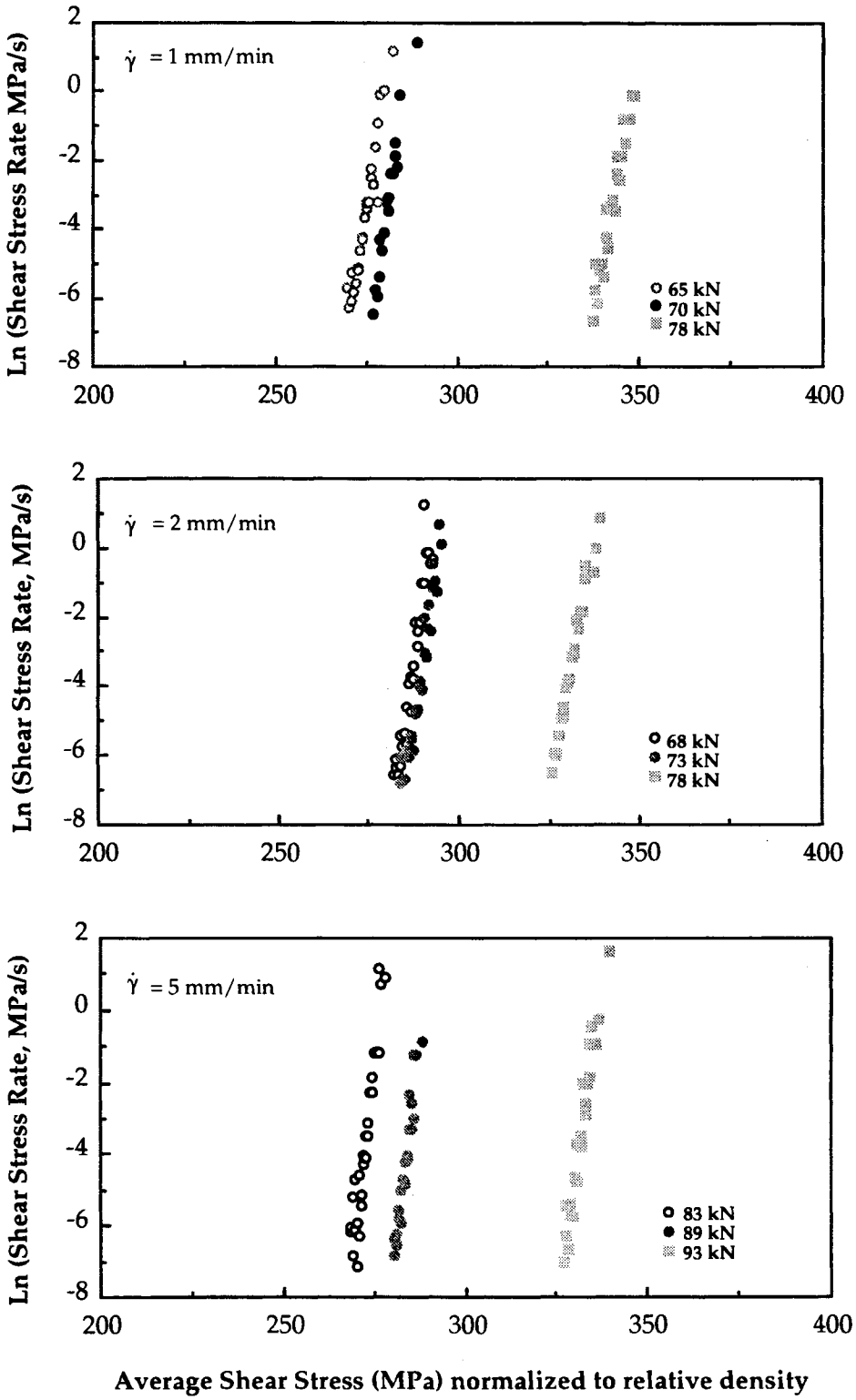

Fig. 5. The ln(shear stress rate) versus average shear stress (normalized to relative density) plots for PMMA/coMAA compacts for various maximum loads and temperatures at strain rates of 1, 2, and 5 mm/min. Normalization does not produce collinearity.

particle-particle contact deformation model of time-dependent compaction which is underway.

ACKNOWLEDGMENTS

The authors would like to gratefully acknowledge the support provided by the Medical Research Council of Canada for this work in the form of a grant (to W. D. H.) and a studentship (to S. L.).

REFERENCES

1. W. C. Duncan-Hewitt. Uniaxial Compaction Modelled using the Properties of Single Crystals. *Drug. Dev. Ind. Pharm.* **19**:2197–2240 (1993).
2. E. A. Papadimitropoulos. *Post consolidation behavior of two crystalline materials, sodium chloride and potassium bromide.* M.Sc. Thesis, University of Toronto, 1990.
3. A. S. Krausz and H. Eyring. *Deformation kinetics,* John Wiley & Sons, New York, 1975.
4. B. Faucher and A. S. Krausz. The Kinetics Analysis of Stress Relaxation. *Phys. Stat. sol. A* **58**:205–212 (1980).
5. W. T. Morehead and E. G. Rippie. Timing Relationships among Maxima of Punch and die-Wall Stress and Punch Displacement during compaction of Viscoelastic solids. *J. Pharm. Sci.* **79**:1020–1022 (1990).
6. E. G. Rippie and D. W. Danielson. Viscoelastic stress/strain behavior of pharmaceutical tablets: Analysis during unloading and post-compression periods. *J. Pharm. Sci.,* **21**:476–481 (1981).
7. E. A. Papadimitropoulos and W. C. Duncan-Hewitt. Predicting the post consolidation relaxation behavior of sodium chloride tablets. *J. Pharm. Sci.* **81**:701–704 (1992).
8. D. M. Marsh. Plastic flow in glass. *Proc. Roy. Soc. A.* **279**:420–435 (1963).
9. J. D. Eshelby. The determination of the elastic field of an ellipsoidal inclusion, and related problems. *Proc. R. Soc. A.* **241**:376 (1957).
10. A. Thierry, R. J. Oxborough, and P. B. Bowden. A molecular model for yield and flow in polymethylmethacrylate. *Philos. Mag.* **30**(3):527–536 (1974).
11. J. D. Ferry. *Viscoelastic Properties of Polymers,* 2nd ed. John Wiley & Sons Inc., New York, 1980. p. 671.
12. E. L. Rodriguez and F. E. Filisko. Temperature Changes in Poly(-Methyl Methacrylate) and High-Density Polyethylene during Rapid compressive Deformation. *Polym. Eng. Sci.* **26**(15):1060–1065 (1986).
13. Z. B. Ahmad and M. F. Ashby. Failure-mechanism maps for engineering polymers. *J. Mater. Sci.,* **23**:2037–2050 (1988).
14. P. B. Bowden and S. Raha. Molecular model for yield and flow in amorphous glassy polymers making use of a dislocation analog. *Philos. Mag.,* **29**:149–166 (1973).
15. M. C. Boyce and E. M. Arruda. An Experimental and Analytical Investigation of the Large Strain Compressive and Tensile Response of Glassy Polymers. *Polym. Eng. Sci.,* **30**:1288–1298 (1990).